On Power System Frequency Control in Emergency Conditions

H. Bevrani†, G. Ledwich*, J. J. Ford* and Z. Y. Dong**

Abstract – Frequency regulation in off-normal conditions has been an important problem in electric power system design/operation and is becoming much more significant today due to the increasing size, changing structure and complexity of interconnected power systems. Increasing economic pressures for power system efficiency and reliability have led to a requirement for maintaining power system frequency closer to nominal value.

This paper presents a decentralized frequency control framework using a modified low-order frequency response model containing a proportional-integral (PI) controller. The proposed framework is suitable for near-normal and emergency operating conditions. An H∞ control technique is applied to achieve optimal PI parameters, and an analytic approach is used to analyse the system frequency response for wide area operating conditions. Time-domain simulations with a multi-area power system example show that the simulated results agree with those predicted analytically.

Keywords: frequency control, power system, robust performance, H∞, emergency condition, frequency response

1. Introduction

Power system frequency regulation, including load-frequency control (LFC) and automatic generation control (AGC), is an ancillary service that plays a fundamental role in supporting power exchanges and providing better conditions for the electricity trading [1]. A simplified frequency regulation mechanism is first introduced in [2], [3], and has since evolved over several decades. There has continued to remain interest in proposing new frequency control approaches with improved ability to maintain system frequency close to nominal value [4].

Following a large generation loss disturbance, a power system's frequency may drop quickly if the remaining generation no longer matches the load demand. System frequency changes in large scale power systems are a direct result of the imbalance between the electrical load and the power supplied by system connected generators. Therefore, system frequency provides a useful index to indicate the system generation and load imbalance. Any short term energy imbalance will result in an instantaneous change in system frequency as the disturbance is initially offset by the kinetic energy of rotating plant. Significant loss of generating plant without adequate system response can produce extreme frequency excursions outside the working range of plant. Off-normal frequency deviations can directly impact on power system operation, system reliability and efficiency. Large frequency deviations can damage equipments, degrade load performance, overload transmission lines, and interfere with system protection schemes. These large-frequency deviation events can ultimately lead to system collapse [5].

Depending on the size of the frequency deviation experienced, LFC, emergency control and natural governor response may all be required to maintain power system frequency. One method of characterizing frequency deviations experienced by a power system is in terms of the frequency deviation ranges and related control actions shown in Table 1. The frequency variation ranges Δf_1, Δf_2, Δf_3 and Δf_4 are identified in terms of different power system operating conditions (perhaps specified in terms of local regulations). Under normal operation, frequency is maintained near to nominal frequency by balancing generation and load. This is, for small frequency deviations up to Δf_1, these deviations can be attenuated by the governor natural autonomous response (primary control). A LFC system can be used to restore area frequency if it deviates more than Δf_1 Hz. In particular, any LFC system must be designed to maintain the system frequency and time deviations within the limits in specified frequency operating standards. The value of Δf_2 is mainly determined by the available amount of operating reserved power in the system [6].

For even larger frequency deviations and in a more complex condition (such as Δf_3 and Δf_4 frequency deviation events) the emergency control and protection schemes must be used to restore the system frequency. There is a risk that these large frequency deviation events might be followed by additional generation events, load/network events, separation events or multiple contingency events.

† School of Engineering Systems, Queensland University of Technology, Australia.(bevrani@qut.edu.au)
* School of Engineering Systems, Queensland University of Technology, Australia.
** School of Information Technology and Electrical Engineering, Australia .(zdong@itee.uq.edu.au)
Received ; 29 February, 2008 Accepted 28 May 2008

The frequency operating standards could be different from network to network. For example in Australia, for the mainland regions, the Δf_1, Δf_2, Δf_3 and Δf_4 are specified as 0.3 Hz, 1 Hz, 2 Hz and 5 Hz, respectively [7]. Further, in the Australian network, the frequency threshold used to start under-frequency load shedding is 49 Hz (50Hz is the nominal system frequency).

Several frequency response models and control scenarios have attempted to address such contingency conditions using emergency control strategies during the past years [8]-[11]. A centralized emergency control approach is used in many of the proposed schemes. Moreover, most published works on the power system frequency regulation have considered separate modelling (and even analysis techniques) for the normal/LFC conditions and emergency conditions.

This paper's key objective is to provide an effective frequency control framework using a more complete frequency response model suitable for wide range of operating conditions. For this purpose a robust PI based control methodology is proposed and a new analytic approach is used to examine the frequency regulation under normal, near-normal and emergency operating conditions.

2. Modified frequency response model

In this paper, a modified dynamical structure is introduced for representing the control area frequency response. This structure represents the effect of emergency control/protection schemes (as well as primary and supplementary control loops). Fig. 1 shows the block diagram of the modified control area model with n generator units.

The shown blocks and parameters are defined as follows: Δf is frequency deviation, ΔP_m is governor valve position, ΔP_S is supplementary control action, ΔP_P is primary control action, ΔP_{tie} is net tie-line power flow, ΔP_{EC} is emergency control/protection action, $\Delta P_{L\text{-}local}$ is local load deviation, ΔP_{UFLS} is under-frequency load shedding effect, ΔP_{UFGT} is under-frequency generation trip effect, ΔP_{OFGT} is over-frequency generation trip effect, H is equivalent inertia constant, D is equivalent damping coefficient, T_j is tie-line synchronizing coefficient with area j, T_g is governor time constant, T_t is turbine time constant, B is frequency bias, v is area interface, R_i is drooping characteristic, ACE is area control error, α_i is participation factors, $M(s)$ is low-order governor-turbine model, and PI is proportional-integral controller.

In comparison of conventional LFC model [2], [3], Fig. 1 shows a more detailed load-frequency response model. Here, to cover the variety of generation types in a control area, different values for turbine-governor parameters and the generator regulation parameters are considered. The frequency performance of a control area is represented approximately by a lumped load generation model using an equivalent frequency, inertia and damping factors [12].

$$\Delta f = \Delta f_{sys} = \sum_{i=1}^{N} (H_i \Delta f_i) / \sum_{i=1}^{N} H_i$$
$$H = H_{sys} = \sum_{i=1}^{N} H_i \quad (1)$$
$$D = D_{sys} = \sum_{i=1}^{N} D_i$$

Table 1. Frequency operating and control actions

Deviation range	Condition	Control action
Δf_1	No contingency or load event	Normal operating
Δf_2	Generation/load or network event	LFC operating
Δf_3	Separation event	Emergency operating
Δf_4	Multiple contingency event	Emergency operating

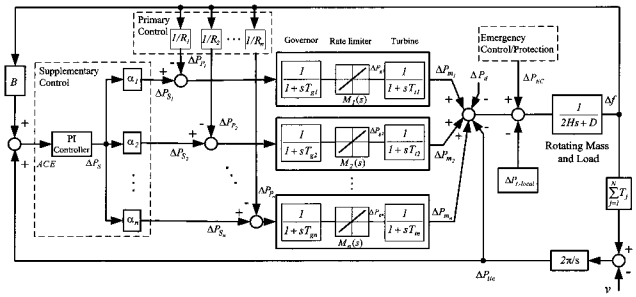

Fig. 1. Modified frequency response model for emergency conditions

If the amount of electrical load in a control area is increased rapidly, due to changes in consumer load demands, then the extra energy required is drawn from the generating units' rotors. These rotors therefore slow down, thus reducing system frequency. For small load changes, the corresponding generation changes can be slower. In the market environment, the system's responses to load changes are provided as regulating ancillary services i.e., LFC or AGC.

Continuing with the example of increased customer load demand, in response to large sudden load changes a rapid increase in generation would be required to initially arrest the decline in system frequency, and to then restore the frequency to the nominal level. For a very large changes in system frequency, such as might arise from a multiple contingency events, the combined response of the generating units' and supplementary control ΔP_S may not be enough, and may not be reliable. Additional

contingency ancillary services or emergency control plans maybe required to avoid market failure and to stop further frequency decline to the point where generating units are beyond their reliable operating limits. For example, it might be reasonable to require customers to make a percent of their load available for such emergency shedding by under-frequency relays. This emergency load shedding would only be used if the frequency falls below the frequency threshold.

The real-world LFC systems usually use proportional integral (PI) controllers [13]. According to Fig. 1, in a control area the ACE performs the input signal for the supplementary control system. Therefore the output signal of the mentioned system has the following form; where K_P and K_I are the constant PI parameters.

$$\Delta P_{S_i}(s) = \alpha_i (K_P + \frac{K_I}{s}) ACE(s) \qquad (2)$$

2.1 Emergency Control/Protection Block

The conventional LFC model gives the free response of the LFC based system following a contingency. In the case of contingency analysis, the emergency protection and control dynamics must be adequately modelled in the frequency response model. Since they directly influence the area power generation/load balance, the mentioned emergency dynamics should be added to the area control system model via the emergency control/protection block shown in Fig. 1.

In the case of a large generation loss disturbance, the available power reserve may not be enough to restore the system frequency and the power system operators may follow an emergency control plan such as under-frequency load shedding (UFLS). The UFLS strategy is designed so as to rapidly balance the demand of electricity with the supply and to avoid a rapidly cascading power system failure. Allowing normal/LFC frequency variations within expanded limits will require the coordination of primary and supplementary controls with generator load set points, for example under-frequency generation trip (UFGT), over-frequency generation trip (OFGT) and other frequency controlled protection devices. According above explanation, we can describe the emergency control/protection block as follows, which is realized in Fig. 2.

$$\Delta P_{EC}(s) = \Delta P_{UFLS}(s) - \Delta P_{UFGT}(s) - \Delta P_{OFGT}(s) \qquad (3)$$

The emergency control schemes and protection devices dynamics are usually represented using incremented/decremented step behaviour. Thus in Fig. 2, the related blocks can be modelled as a sum of incremental (decremental) step functions. For a fixed UFLS scheme [8], the function of ΔP_{UFLS} in time domain could be considered as a sum of incremental step functions of $\Delta P_j u(t-t_j)$. Therefore, for L load shedding steps we have

$$\Delta P_{UFLS}(t) = \sum_{j=0}^{L} \Delta P_j \, u(t-t_j) \qquad (4)$$

where ΔP_j and t_j denote the incremental amount of load shed and time instant of the jth load shedding step, respectively. Similarly, to formulate the ΔP_{OFGT} and ΔP_{UFGT}, we can use appropriate step functions. Therefore using the Laplace transformation, is it possible to represent $\Delta P_{EC}(s)$ in following summarized form

$$\Delta P_{EC}(s) = \sum_{l=0}^{N} \frac{\Delta P_l}{s} e^{-t_l s} \qquad (5)$$

where ΔP_l is the size of equivalent step load changes due to generation/load event or a load shedding scheme at t_l.

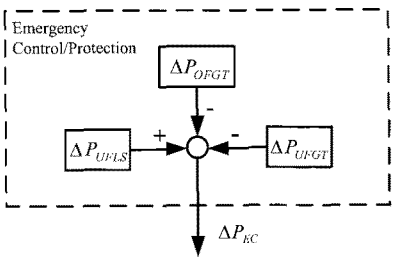

Fig. 2. Emergency control/protection block Remark:

Generally, frequency stability problems are associated with inadequacies in equipment responses, poor coordination of control and protection equipment, or insufficient generation reserve. The frequency stability may be a short-term phenomenon or a long-term phenomenon. During frequency excursions, the characteristic times of the processes and devices that are activated will range from fraction of seconds, corresponding to the response of devices such as UFLS and generator controls and protections, to several minutes, corresponding to the response of devices such as prime mover energy supply systems and load voltage regulators [14].

Here it is assumed that the emergency control/protection dynamics are not much slow, and are comparable with the LFC cycle rates. Otherwise, the LFC dynamic response should not be taken into account in emergency control schemes and their analysis ($\Delta P_s = 0$). In other words, the introduced modified LFC model is suitable for the emergency control dynamics in the range of a few seconds to several minutes.

3. Robust Tuning of PI Controller

Optimal tuning of PI controller ensures a smooth coordination between generator set-point signals and the

scheduled operating points. Usually, the PI controllers in real-world LFC systems are tuned online based on classical and trial-and-error approaches. During the last decade, several decentralized control methodologies have been developed to design of PI based LFC system [13], [15], [16]. Most published research works have neglected problems associated with the communication network. This was a valid assumption in the case of traditional dedicated communication links however the use of an open communication infrastructure to support the ancillary services in deregulated environments raises concerns about problems that may arise in the communication system.

In this section, the PI control problem (for the supplementary closed loop) is transferred to a static output feedback (SOF) control design problem where we can consider tuning of PI parameters in the presence of time delays, using an optimal H∞ control formulation and a multi constraint minimization problem. The problem formulation is based on expressing the constraints as LMI which can be easily solved using available semidefinite programming methods [17].

3.1 Problem Formulation

Consider the open-loop state space model of a control area in the following time-delayed system form:

$$\begin{aligned} \dot{x}(t) &= Ax(t) + Bu(t) + A_d x(t-d) + B_h u(t-h) + Fw(t) \\ z(t) &= C_1 x(t) \\ y(t) &= C_2 x(t) \end{aligned} \tag{6}$$

Here $x \in \Re^n$ is the state vector, $C_2 \in \Re^n$ is the constant matrix such that the pair (A, C_2) is detectable. d and h represent the delay amounts in the state and the input respectively. $A \in \Re^{n\times n}$ and $B \in \Re^{n\times m}$ represent the nominal system without delay such that the pair (A, B) is stabilizable. $A_d \in \Re^{n\times n}$, $B_h \in \Re^{n\times m}$, $F \in \Re^{n\times q}$ are known matrices and $\psi(t)$ is a continuous vector-valued initial function.

For purposes of this work, the communication delays are considered on the control input and control output of the supplementary control loop: the delays on the measured frequency and power tie-line flow from remote terminal units (RTUs) to PI controller which can be considered on the ACE signal and the produced rise/lower signal from controller to individual generation units.

Recalling Fig. 1, the PI control design problem can be transferred to a static output feedback (SOF) control problem by augmenting the measured output signal to include the area control error (ACE) and its integral [13], [15].

$$u(t) = ky(t) \tag{7}$$

$$u(t) = K_P ACE + K_I \int ACE = [K_P \quad K_I]\left[ACE \quad \int ACE\right]^T \tag{8}$$

The overall control framework to formulate the time-delayed PI control problem via an H∞ based SOF (H∞-SOF) control design is shown in Fig. 3. Here $G(s)$ is the nominal dynamic model of the given control area, u is the control input and w includes the perturbed and disturbance signals in the given control area. The output channel z_∞ is associated with the H∞ performance while the y is the augmented measured output vector (ACE and its integral). Also, μ_1, μ_2 and μ_3 are constant weights that must be chosen by designer to get the desired closed-loop performance. The first two terms of z_∞ output are used to minimize the effects of disturbances on area frequency and area control error by introducing appropriate fictitious controlled outputs. Furthermore, fictitious output $\mu_3 \Delta P_S$ sets a limit on the allowed control signal used to penalize fast changes and large overshoot in the governor load set-point with regards to practical constraint on power generation by generator units [18].

Using the block diagram of Fig. 1 and consistent with the standard dynamic model for the prime mover and governor in a control area [19], the state variables of $G(s)$ in (6) can be determined as follows:

$$x^T = [\Delta f \quad \Delta P_{tie} \quad \int ACE \quad x_m \quad x_g] \tag{9}$$

where

$$\begin{aligned} x_m &= \left[\Delta P_{m1} \quad \Delta P_{m2} \quad \cdots \quad \Delta P_{mn}\right] \\ x_g &= \left[\Delta P_{g1} \quad \Delta P_{g2} \quad \cdots \quad \Delta P_{gn}\right] \end{aligned} \tag{10}$$

and

$$\begin{aligned} y^T &= [ACE \quad \int ACE], u = \Delta P_S, w^T = [\Delta P_D \quad v] \\ z_\infty^T &= \left[\mu_1 \Delta f \quad \mu_2 \int ACE \quad \mu_3 \Delta P_S\right] \end{aligned} \tag{11}$$

3.2 Optimal H∞ based PI Controller

Using the described transformation from PI to SOF control design, the time-delayed PI control problem is reduced to the synthesis of a SOF controller for the time-delay system (6) of the form of (7). Here k is a static gain vector to be determined.

A variety of SOF problems have been studied by many researchers, and many analytical and numerical methods for local/global solutions have been discussed [20], however only few references have addressed this design problem for time delayed systems.

In this paper, in order to obtain an optimal LMI-based H∞ solution for the problem at hand, the following

theorem is used. This theorem adapts H∞ theory with time-delayed systems (using LMI description) and establishes the conditions under which the SOF control law (7) stabilizes (6) and guarantees the H∞ norm bound γ of the closed-loop transfer function T_{zw}, namely $\|T_{zw}\|_\infty < \gamma$; $\gamma > 0$.

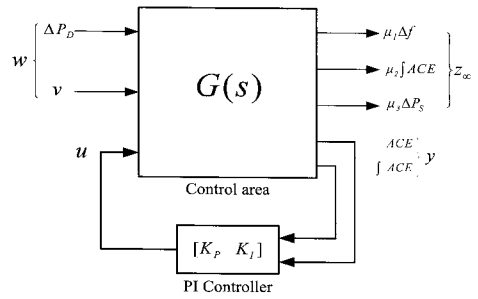

Fig. 3. H∞-SOF control framework

Theorem: The SOF controller k asymptotically stabilizes the system (6) and $\|T_{zw}\|_\infty < \gamma$ for $d, h \geq 0$ if there exist matrices $0 < Y^T = Y \in \Re^{n\times n}$, $0 < Q_t^T = Q_t \in \Re^{n\times n}$ and $0 < Q_s^T = Q_s \in \Re^{n\times n}$ satisfying the matrix inequality (12).

$$[AY+YA^T+Q_t+Q_s]+[BkC_2(BkC_2)^T+Y^TY]+[A_dYQ_s^{-1}(A_dY)^T] \\ +[B_hkC_2YQ_s^{-1}(B_hkC_2Y)^T]+YC_1^TC_1Y+\gamma^{-2}FF^T<0 \quad (12)$$

Proof is given in [21]. The LMI problem (12) is convex and can be solved efficiently using the LMI Control Toolbox [22]. The present robust tuning methodology is much simpler than the addressed robust PI/PID tuning techniques in [23], [24].

4. Frequency Response: An Analytic Approach

4.1 Frequency Response

Using the modified model, the system frequency can be obtained as follows.

$$\Delta f(s) = \frac{1}{2Hs+D}[\Delta P_m(s) + \\ \Delta P_{EC}(s) - \Delta P_{tie}(s) - \Delta P_{L\text{-}local}(s) - \Delta P_d] \quad (13)$$

where

$$\Delta P_m(s) = \sum_{i=0}^{n} \Delta P_{mi}(s) \quad (14)$$

$$\Delta P_{m_i}(s) = M_i(s)\Delta P_{C_i}(s) \quad (15)$$

Here

$$\Delta P_{C_i}(s) = \Delta P_{S_i}(s) - \Delta P_{P_i}(s) \quad (16)$$

$$\Delta P_{P_i}(s) = \frac{\Delta f(s)}{R_i} \quad (17)$$

$$\Delta P_{S_i}(s) = \alpha_i(K_P + \frac{K_I}{s})(\Delta P_{tie}(s) + \beta\Delta f(s)] \quad (18)$$

Practically, the integral coefficient K_I is enough small and can be ignored in the computation. The expressions (2), (3), (15), (16), (17) and (8) can be substituted into (13) with the result

$$\Delta f(s) = \frac{1}{2Hs+D}([K_P\sum_{i=1}^{n}\alpha_iM_i(s) - 1]\Delta P_{tie}(s) \\ -[\sum_{i=1}^{n}M_i(s)(\frac{1}{R_i} - \alpha_i\beta K_P]\Delta f(s) + \\ \sum_{l=0}^{N}\frac{\Delta P_l}{s}e^{-t_ls} - \Delta P_{L\text{-}local}(s) - \Delta P_d) \quad (19)$$

For the sake of load disturbances analysis we are usually interested to model load disturbance and local demand changes in the form of a step function, i.e.,

$$\Delta P_{L\text{-}local}(s) - \Delta P_d = \frac{\Delta P_d}{s} \quad (20)$$

Substituting (20) in (19) and summarizing the result yields

$$\Delta f(s) = \frac{g_2(s)}{g_1(s)}\Delta P_{tie}(s) + \frac{1}{sg_1(s)}(\sum_{l=0}^{N}\Delta P_l\, e^{-t_ls} - \Delta P_d) \quad (21)$$

where

$$g_1(s) = 2Hs + D + \sum_{i=1}^{n}M_i(s)(\frac{1}{R_i} - \alpha_i\beta K_P) \quad (22)$$

and

$$g_2(s) = K_P\sum_{i=1}^{n}\alpha_iM_i(s) - 1 \quad (23)$$

$$M_i(s) = \frac{1}{(1+T_{gi}s)}\cdot\frac{1}{(1+T_{ti}s)} \quad (24)$$

Substituting $M_i(s)$ from (24) in (22) and (23), and using the final value theorem, the frequency deviation in steady state (Δf_{ss}) can be obtained from (19).

$$\Delta f_{ss} = \lim_{s\to 0} s.\Delta f(s) = 0 + \frac{1}{D + \sum_{i=1}^{n}\frac{1}{R_i} - \beta K_P\sum_{i=1}^{n}\alpha_i}(\sum_{l=0}^{N}\Delta P_l - \Delta P_d) \quad (25)$$

By definition [1], system's frequency response

characteristic (β) is equivalent to

$$\beta = D + \frac{1}{R_{sys}} \tag{26}$$

and considering

$$\sum_{i=1}^{n} \alpha_i = 1 \quad ; \quad 0 \le \alpha_i \le 1 \tag{27}$$

$$\sum_{i=1}^{n} \frac{1}{R_i} = \frac{1}{R_{sys}} \tag{28}$$

the equation (25) can be rewritten into the following form

$$\Delta f_{ss} = -\frac{\Delta P_D}{(D + \frac{1}{R_{sys}})(1 - K_P)} \tag{29}$$

where

$$\Delta P_D = \Delta P_d - \sum_{i=0}^{N} \Delta P_i \tag{30}$$

Since the value of droop characteristic R_i is generally bounded between about 0.05 and 0.1 for most generator units ($0.05 \le R_i \le 0.1$) [9], for a given control system according to (28) we can write

$$R_{sys} \le R_{i,\,min} \tag{31}$$

and for a small enough DR_{sys}, (29) can be reduced to

$$\Delta f_{ss} = -\frac{R_{sys}\Delta P_D}{(DR_{sys} + 1)(1 - K_P)} \cong -\frac{R_{sys}\Delta P_D}{(1 - K_P)} \tag{32}$$

4.2 Total Load Change Estimation

As previously mentioned, frequency changes can induce a corresponding change in demand load. This effect is called load relief and should be taken into account when calculating the amount of required ancillary service [25]. The change in demand is always in a direction that tends to alleviate the frequency deviation. i.e., for a reduction in frequency, the load relief is negative (decrease in demand), which tends to alleviate the falling frequency. In the mainland part of the Australian power network, for every 1% change in frequency (0.5 Hz) it is assumed there will be a corresponding 1.5% change in demand [25].

From (32), the magnitude of ΔP_D can be estimated as follows.

$$\Delta P_D = -\frac{(1 - K_P)}{R_{sys}} \Delta f_{ss} \tag{33}$$

To compensate the power imbalance ΔP_D , the total necessary secondary regulation should be

$$\Delta P_S = -\Delta P_D = \frac{(1 - K_P)}{R_{sys}} \Delta f_{ss} \tag{34}$$

For the sake of dynamic frequency analysis in the presence of sudden load changes, it is usual to model the multi machine dynamic behaviour by an equivalent single machine [9]. Using the concept of an equivalent single machine, we can simplify the control area block diagram (Fig. 1) as shown in Fig. 4. Here, ΔP_D covers the effect of local load disturbance, local demand and tie-line power changes, and, network and generation events.
According to Fig. 4, we can write

$$\Delta f(s) = \frac{-1}{2Hs + D} \Delta P_D(s) \tag{35}$$

or

$$\Delta P_D(t) = -2H \frac{d\Delta f(t)}{dt} - D\Delta f(t) \tag{36}$$

Comparing the magnitude of total load change in (33) and (36), the area average frequency during a sampling period T_S , can be estimated as following difference equation:

$$\Delta f(T_S) = \frac{2HR_{sys}}{T_S(1 + K_P)}[\Delta f(t_1) - \Delta f(t_0)] + \frac{DR_{sys}}{(1 + K_P)} \Delta f(t_1) \tag{37}$$

where the t_0 and t_1 are boundary samples within the assumed interval. The result can be used in (33) to calculate the size of ΔP_D .

$$\Delta P_D = -\frac{2H}{T_S}[\Delta f(t_1) - \Delta f(t_0)] - D\Delta f(t_1) \tag{38}$$

For a control area with a small enough damping factor, (38) can be approximated as follows.

$$\Delta P_D \approx -\frac{2H}{T_S}[\Delta f(t_1) - \Delta f(t_0)] \tag{39}$$

Thus, the frequency gradient in a control area is proportional to the magnitude of overall disturbance in that area. This result agrees with the obtained results in other published works [26]. The factor of proportionality is the system inertia H. Actually the inertia constant is loosely defined by the mass of all the synchronous

rotating generators and motors connected to the system. For a specific load decrease, if H is high, then the frequency will fall slowly and if H is low, then the frequency will fall faster.

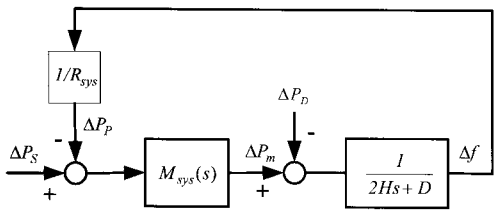

Fig. 4. Simplified control area model

5. Application to 3-Control Area Power System

5.1 Configuration of Study System

To illustrate the effectiveness of the proposed control strategy and developed analytic approach, a nonlinear simulation has been performed. A power system with three control areas, shown in Fig. 5, is used. Each control area has some generator units and, at the same time, is connected to other areas. The power system parameters are considered the same as given in [27]. It is assumed that each control area is responsible to maintain its frequency close to a specified nominal value.

5.2 PI Parameters

To adapt (6) with the structure of time-delayed power system [28], the A_d and B_h can be computed by transferring the delays on ACE signal (τ_d) and ΔP_S signal (τ_h) through their components (Δf , ΔP_{tie} and u). The coefficients μ_1 , μ_2 and μ_3 set the frequency control performance goals (tracking the load variation, disturbance attenuation and putting physical limits on control action signal). For the study system at hand, the total time delays of communication channels is assumed to be similar to the LFC cycle rate of the power system and suitable values for the weights μ_1, μ_2 and μ_3 are chosen as 0.5, 1 and 5, respectively. According to the synthesis methodology described in Sections 3, the parameters of PI controllers for the three control area are obtained as follows.

$$\begin{aligned} K_{P1} &= -0.3061, \quad K_{I1} = -0.0243 \\ K_{P2} &= -0.1059, \quad K_{I2} = -0.0150 \\ K_{P3} &= -0.4160, \quad K_{I3} = -0.0103 \end{aligned} \tag{40}$$

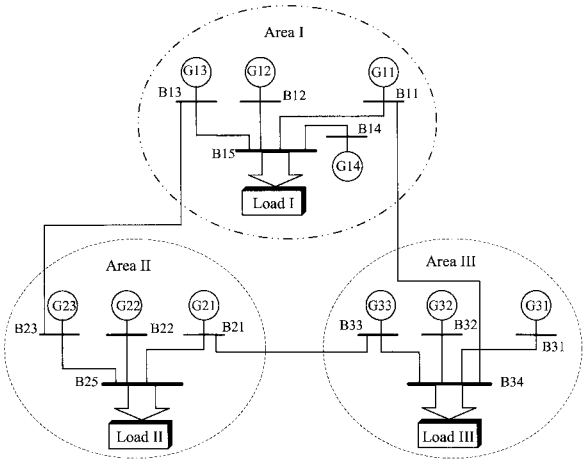

Fig. 5. 3-Control area power system

Based on the given theorem in Section 3, since the design basis of the SOF controller (7) is to simultaneously stabilize (6) and guarantee the H∞-norm bound γ of the closed-loop transfer function T_{zw}, namely,

$$\|T_{zw}\|_\infty < \gamma \quad ; \quad \gamma > 0 \tag{41}$$

the designed PI controllers ensure that the closed-loop system properly satisfies this robustness condition.

5.3 Simulation Results

It is assumed that the maximum reserved LFC power ΔP_{Rmax} in each area available to track power imbalance is fixed at 100 MW. For the first scenario, the system frequency response is tested following a step loss of generation 0.1 pu in area-1, with simultaneous increase of 0.02 pu load steps in area-2 and area-3. The frequency deviation, the corresponded frequency gradient, and the output of PI controllers for three control areas are shown in Fig. 6. The higher frequency rate changes occur in area-1. Recalling (39), since the disturbance magnitude in area-1 was higher than the other areas, this behaviour is easily understandable. The rate of frequency change is proportional to the power imbalance, and it also depends on the area system inertia. From Fig. 6, it can be concluded that the disturbance location affects the frequency behaviour of power systems and consequently the design and selection of a suitable emergency control plan.

In steady state, the frequency deviation (Δf_{ss}) reaches the value given by (29). Since the frequency deviations remained within near-normal frequency operating bound (Δf_1 and Δf_2) and the available power reserve (100 MW) is sufficient to match the power demand, the system recovered within 15 seconds. Fig. 7 shows the total mechanical power change in each control area for the mentioned test scenario. The obtained results show that

the designed PI controllers can ensure good performance despite load disturbances, and properly act to maintain area frequency and total exchange power close to the scheduled values (by sending corrective smooth signals to the generators in proportion to their participation in the frequency regulation task).

After the primary (governor) response, the supplementary control responds by using the available instantaneous reserve to raise the frequency back to the nominal level. However, following disturbances of large magnitude, or when there is not enough reserved power, the frequency (in steady state) may not return to a normal operating condition.

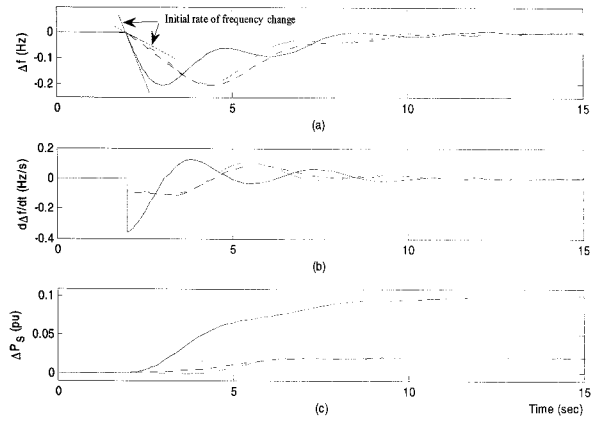

Fig. 6. System response for scenario 1; a) frequency deviation, b) frequency gradient and c) PI control signal. Area-1 (solid), area-2 (dotted) and area-3 (dashed-line)

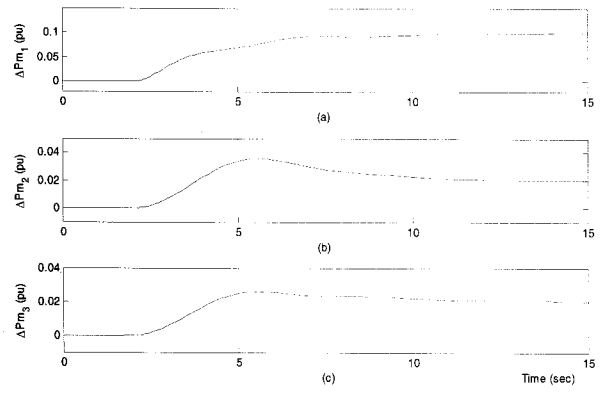

Fig. 7. Mechanical power change for scenario 1; a) area-1, b) area-2, and c) area-3.

Consider the system frequency response following a more sever condition: simultaneous applying 0.3 pu, 0.05 pu and 0.05 pu load disturbance in area-1, area-2 and area-3, respectively. In the present test case (scenario 2), the total area load demand is much higher than the ΔP_{Rmax} in control areas. As shown in Fig. 8, the primary and supplementary controls are not able to maintain the frequency at the nominal value and the steady state frequency may pass the threshold frequency f_t. The Δf_{ss} in each control area, can be analytically calculated using (32).

We can use (33) to assess whether the frequency passes the frequency threshold and whether emergency control action may be necessary. According to (33), the maximum amount of available area power reserve ΔP_{Rmax} can compensate the following steady state area frequency deviation.

$$\Delta f_{max} = \left| \frac{R_{sys}}{(1-K_P)} \Delta P_{Rmax} \right| \tag{42}$$

Therefore, the load shedding frequency threshold, which can be determined as follows.

$$f_t = f_0 - \Delta f_{max} = f_0 - \left| \frac{R_{sys}}{(1-K_P)} \Delta P_{Rmax} \right| \tag{43}$$

In a realistic multi-area power system, there must be sufficient reserve from the energy market to ensure that no more than a small percent of annual customer demand is at risk of not being supplied (in Australian power network the limit is considered to be 0.002 per cent risk of no supply). The reserve margins for each region of the market must be calculated appropriately.

For example in Australian network, NEMMCO determined the following reserve margins, which applied from late in June 2004: Queensland 610 MW; New South Wales -290 MW; and 530 MW of reserve shared across the combined regions of Victoria and South Australia, provided that 265 MW of this amount is available within South Australia [29].

Continuing with the simulation example, assume that the frequency has passed the load shedding frequency threshold f_t and thus UFLS emergency control actions are needed to recover the system frequency. In this case, the system is in an emergency condition and we need to follow a suitable load disconnection (load shedding) procedure to recover the system frequency. Considering the overall area load disturbance magnitude (33), a three staged load shedding plan is investigated and started at 20 s (Fig. 9). The loads 0.1 pu, 0.05 pu and 0.05 pu are disconnected in control area-1 at 20 s, 35 s and 45 s, respectively.

$$\Delta P_{UFLS}(t) = 0.1u(t-20) + 0.05u(t-35) + 0.05u(t-45) \tag{44}$$

The frequency deviation and its derivative during the emergency operating conditions are shown in Fig. 9.

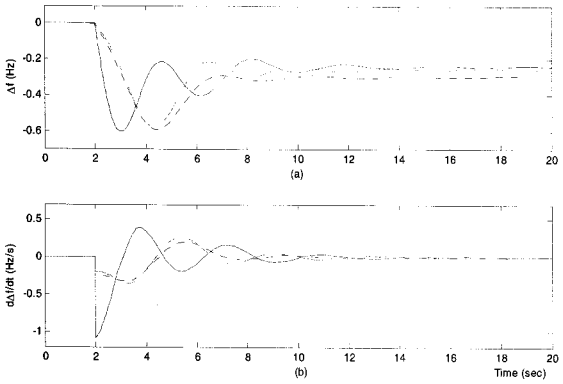

Fig. 8. System response for scenario 2 (without emergency control action); a) frequency deviation, and b) frequency gradient. Area-1 (solid), area-2 (dotted) and area-3 (dashed-line).

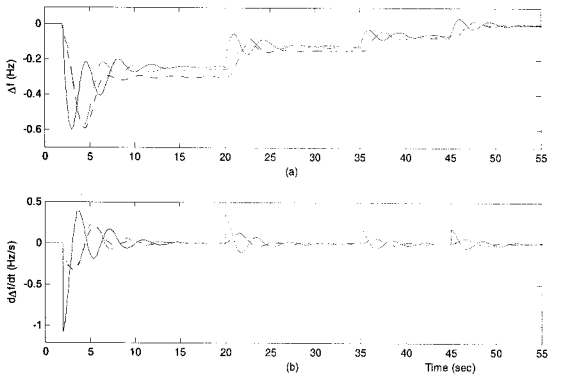

Fig. 9. Applied UFLS to recover the area frequency for scenario 2

6. Conclusion

This paper introduced a modified frequency response model suitable for synthesis and analysis of power system frequency control problem in near-normal and contingency conditions. The effects of emergency control/protection dynamics are properly considered. The PI based frequency control problem is formulated as a robust H∞-SOF optimization control problem. An analytic approach is introduced to analyze the area frequency response following load disturbances. Finally, the analytical results are examined using nonlinear simulation of a three control area power system.

Acknowledgements

This work is supported by Australian Research Council (ARC) under grant DP0559461.

References

[1] P. Kundur, Po*wer system stability and control*, Englewood Cliffs, NJ: McGraw-Hill, 1994.

[2] O. I. Elgerd, C. Fosha, "Optimum megawatt-frequency control of multiarea electric energy systems," *IEEE Trans. Power Apparatus & Systems*, Vol. PAS-89, No. 4, pp. 556-563, 1970.

[3] C. Fosha, O. I. Elgerd, "The megawatt-frequency control problem: a new approach via optimal control," *IEEE Trans. Power Apparatus & Systems*, Vol. PAS-89, no. 4, pp. 563-577, 1970.

[4] Ibraheem, P. Kumar, and P. Kothari, "Recent philosophies of automatic generation control strategies in power systems," *IEEE Transactions on Power Systems,* Vol. 20, No. 1, pp. 346-357, February, 2005.

[5] B. J. Kirby, J. Dyer, C. Martinez *et al.*, *Frequency control concerns in the North American Electric Power System,* ORNL/TM-2003/41, 2002, Available on-line at http://www.ornl.gov/sci/btc/apps/ Restructuring/ ORNLTM200341.pdf.

[6] H. Bevrani, *Decentralized robust load-frequency control synthesis in restructured power systems*. PhD dissertation, Osaka University, Japan, 2004.

[7] NEMMCO, *Frequency & time deviation monitoring in NEM*, Vol. 2007, NEMCO, 2007, Available on-line at http://www.nemmco.com.au/powersystemops/250-0069.pdf.

[8] D. L. H. Aik, "A general-order system frequency response model incoporating load shedding: analytic modeling and applications," *IEEE Transactions on Power Systems,* Vol. 21, No. 2, pp. 709-717, May, 2006.

[9] P. M. Anderson, and M. Mirheydar, "A Low-Order System Frequency Response Model," *IEEE Transactions on Power Systems,* Vol. 5, No. 3, pp. 720-729, 1990.

[10] M. B. Djukanovic, D. P. Popovic, D. J. Sobajic *et al.*, "Prediction of power system frequency response after generator outages neural nets," *IEE Proceedings-C,* Vol. 140, No. 5, pp. 389-398, September, 1993.

[11] Q. Zhao, and C. Chen, "Study on a system frequency response model for a large industrial area load shedding," *Electrical Power and Energy Systems,* Vol. 27, pp. 233–237, 2005.

[12] P. M. Anderson, and A. A. Fouad, *Power system control and stability*, Piscataway, NJ: IEEE Press, 1994.

[13] H. Bevrani, Y. Mitani and K. Tsuji, "Robust decentralized load-frequency control using an iterative linear matrix inequalities algorithm," *IEE Proc. Gener. Transm. Distrib.*, Vol. 150, No. 3, pp. 347-354, 2004.

[14] P. Kundur, J. Paserba, v. Ajjarapu, et al, "Definition and classification of power system stability," *IEEE Transactions on Power Systems,* Vol. 19, No. 2, pp. 1387-1401, 2004.

[15] D. Rerkpreedapong, A. Hasanovic and A. Feliachi, "Robust load frequency control using genetic algorithms and linear matrix inequalities," *IEEE Transactions on Power Systems,* Vol. 18, No. 2, pp. 855-861, 2003.

[16] C. F. Juang, C. F. Lu, "Load-frequency control by hybrid evolutionary fuzzy PI controller," *IEE Proc. Gener. Transm. Distrib.*, Vol. 2, No. 153, pp. 196-204, 2006.

[17] S. Boyd, L. El. Ghaoui, E. Feron and V. Balakrishnan, *Linear Matrix Inequalities in Systems and Control Theory*, SIAM Books, Vol. 15, Philadelphia, 1994.

[18] N. Jaleeli, D. N. Ewart and L. H. Fink, "Understanding automatic generation control," *IEEE Trans. Power Syst.*, Vol. 7, No. 3, pp. 1106-1112, 1992.

[19] A. J. Wood and B. F. Wollenberg, *Power generation operation and control.* NewYork: Wiley, 1984.

[20] V.L. Syrmos, C.T. Abdallah, P. Dorato, and K. Grigoriadis, "Static output feedback: A survey," *Automatica*, Vol. 33, no. 2, pp. 125-137, 1997.

[21] H. Bevrani, T. Hiyama "Robust load-frequency regulation: a real-time laboratory experiment," Optimal *Control Applications and Methods*, Vol. 28, No. 6, pp. 419-433, 2007.

[22] P. Gahinet, A. Nemirovski, A. J. Laub and M. Chilali, *LMI Control Toolbox*, The MathWorks, Inc., 1995.

[23] H. Bevrani, T. Hiyama "Multiobjective PI/PID control design using an iterative linear matrix inequalities algorithm," *Int. Journal of Control, Automation and Systems*, Vol. 5, No.2, pp. 117-127, April, 2007.

[24] H. Bevrani, T. Hiyama, and Y. Mitani "Power system dynamic stability and voltage regulation enhancement using an optimal gain vector," *Control Engineering Practice*, Vol. 16, No. 9, pp. 1109-1119, 2008.

[25] NEMMCO, *FCAS Constraints*, NEMMCO, 2006, Available on-line at http://www.nemmco.com.au/ancillary_services/160-0272.pdf

[26] J. S. Thorp, X. Wang, K. M. Hopkinson *et al.*, "Agent technology applied to the protection of power systems," *Autonomous systems and Intelligent agents in power system control and operation*, C. Rehtanz, ed., pp. 113-154, Berlin Heidelberg: Springer, 2003.

[27] J. J. Ford, H. Bevrani, G. Ledwich, "Adaptive load shedding and regional protection," To be appeared in *European Trans. on Electrical Power.*

[28] H. Bevrani, T. Hiyama "A control strategy for LFC design with communication delays," In Proceeding of the 7^{th} *Int. Power Engineering Conf. (IPEC)*, Singapore, Dec. 2005.

[29] NECA, "Reliability standards," 2004, Available on-line at http://www.neca.com.au/SubCategory7127.html?SubCategoryID=114.

H. Bevrani

He received the M.Eng. (Hons.) and Ph.D. degrees in Electrical Engineering from K. N. Toosi University of Technology (Iran, 1997) and Osaka University (Japan, 2004), respectively. Currently, he is a research fellow at Queensland University of Technology and an A/professor at University of Kurdistan. His special fields of interest include robust load-frequency control and robust/intelligent control applications in Power system and Power electronic industry.

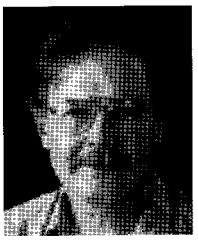

G. Ledwich

He received the Ph.D. degree in electrical engineering from the University of Newcastle, Australia, in 1976. He is a Professor of electrical power engineering at the Queensland University of Technology, Brisbane, Australia. His Professorial Chair has been sponsored since December 1998 by the Transmission and Distribution companies of Queensland. His interests are in the areas of power systems, power electronics and control. Dr. Ledwich is a Fellow of I.E.Aust.

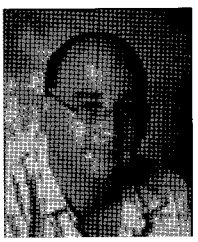

J. J. Ford

He received BSc, BE and PhD degrees from the Australian National University (in 1995, 1995 and 1998 respectively). He is currently a lecturer at the Queensland University of Technology. Previously he has held positions at the University of New South Wales at the Australian Defence Force Academy and at the Defence Science and Technology Organisation. His current research interests include emergency control of power systems, non-linear optimal control and dynamic programming.

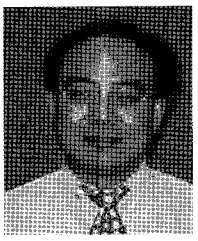

Z. Y. Dong

He obtained his PhD from The University of Sydney, Australia in 1999. He is now an associate professor at the School of Information Technology and Electrical Engineering, The University of Queensland, Australia. His research interest includes power system security analysis, power system planning and management, and power system stability, electricity market, computational intelligence and its application in electric power engineering.